Symmetries in Transmission Electron Microscopy images of semiconductor nanostructures with strain

Anieza Maltsi*, Alexander Mielke*† and Thomas Koprucki*
*Weierstraß-Institut für Angewandte Analysis und Stochastik, Berlin, Germany.
†Humboldt-Universität zu Berlin, Institut für Mathematik, Berlin, Germany.
Email: anieza.maltsi@wias-berlin.de

***Abstract*—Transmission electron microscopy is often used to image semiconductor nanostructures with strain. The resulting images exhibit symmetries, the source of which is not always known. We prove mathematically that the intensities are invariant under specific transformations, which allows us to distinguish between symmetries of the imaging process itself and symmetries of the inclusion.**

I. Introduction

The main goal of transmission electron microscopy (TEM) is to extract information on the specimen from the generated TEM images. This is particularly used for detecting shapes, sizes and composition of inclusions in a larger specimen consisting of a regular crystalline material, like quantum wells and quantum dots. However, there is no direct way to infer the geometric properties of the inclusion from the image, due to the highly non linear behavior of the dynamic diffraction. Hence, a commonly taken approach is to simulate the imaging process with inclusions described by parametrized data. Then, the comparison with experimental pictures can be used to fit the chosen parameters and deduce the desired data of the experimental inclusions [1].

An important feature in this process are symmetries, which may occur in the imaging, for two reasons; first the inclusions may have certain symmetries and second the TEM images may display symmetries that are related but not identical. The latter arise from the fact that the experimental setup may have its own intrinsic symmetry properties, like classical reciprocity relations in scattering [2]. We analyze these symmetries and explain why sometimes TEM images look more symmetric than the inclusion under investigation [3].

II. Modeling and Simulation of TEM images

The simulation of realistic TEM images can be a challenging problem. They are highly sensitive to strain and in order to simulate images similar to experimental ones elasticity theory is required to obtain the strain profile. The strains coming from elasticity are then inserted in the equations describing the propagation of electron beams through the crystal, known as the Darwin–Howie–Whelan (DHW) equations, see [4].

The research was partially supported by the DFG through the Berlin Mathematics Research Center MATH+ (EXC-2046/1, project ID: 390685689) via the subproject EF3-1 *Model-based geometry reconstruction from TEM images.*

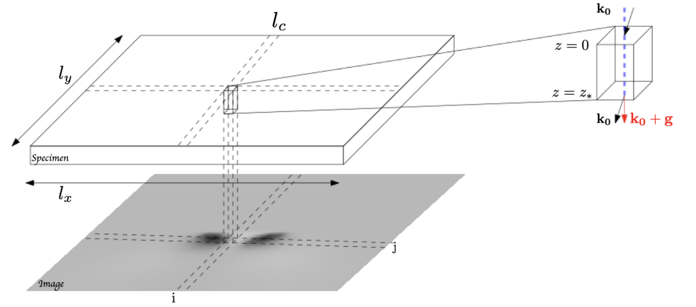

Fig. 1. Column approximation: An incoming beam is assumed not to leave a column centered at the entering point. For this column the intensity of the corresponding pixel is obtained by propagating the beam along a line scan (blue line) in z-direction at position (x_i, y_j) to the exit plane. Image from [3] used under CC-BY.

A toolchain to simulate TEM images by coupling elasticity solutions with the DHW equations is described in [1].

Here we will focus on interpreting symmetries observed in TEM images by analyzing mathematically the DHW equations. While these equations are typically formulated for infinitely many beams in the dual lattice Λ^*, for all practical purposes it is sufficient to use only a few important beams, the so-called m-beam models with wave vectors $\mathbf{g} \in \Lambda^*_m$, because at high energy and for thin specimens only very few beams are excited by scattering of the incoming beam. A mathematical analysis of the corresponding beam selection is given in [5].

Assuming that the crystallographic lattice stays approximately intact and can be modeled as a strained crystal where the positions of the lattice points undergo a displacement $\mathbf{u}(x, y, z)$, the DHW equations for strained crystals can be written in matrix form as:

$$\dot{\phi} := \frac{\mathrm{d}}{\mathrm{d}z}\phi = \mathrm{i}\left(A + F(z)\right)\phi \quad \text{and} \quad \phi(0) = e_{\mathbf{0}} \in \mathbb{C}^m, \quad (1)$$

where the vector $\phi = (\phi_{\mathbf{g}})_{\mathbf{g}\in\Lambda^*_m} \in \mathbb{C}^m$ contains the relevant wave functions $\phi_{\mathbf{g}}$ of the beam associated with wave vector $\mathbf{g} \in \Lambda^*_m$, with $\mathbf{g} = \mathbf{0}$ denoting the incoming beam [3].

The system matrix $A = V + \Sigma$ includes the influence of the electrostatic interaction potential V and the so-called excitation errors $\Sigma = \mathrm{diag}(s_{\mathbf{g}})$, which are experimental parameters that can easily be controlled, e.g by tilting the sample. The elastic displacement $\mathbf{u}$ enters DHW (1) via the *strain profile* $F(z) = \mathrm{diag}(\mathbf{g} \cdot \frac{\mathrm{d}}{\mathrm{d}z}\mathbf{u}(x, y, z)) \in \mathbb{R}^{d\times d}$, which

contains the projections of the strains to the individual wave vectors $\mathbf{g} \in \Lambda_m^*$. The vertical coordinate $z \in [0, z_*]$ gives the depth inside the specimen ($z = 0$ entry plane and $z = z_*$ exit plane), whereas the horizontal coordinates (x, y) are fixed and correspond to the image pixel, see Fig. 1.

In Fig. 2 we see simulated TEM images for a pyramidal quantum dot for different choices of the vector $\mathbf{g}$, illustrating the sensitivity of TEM images to different components of the displacement.

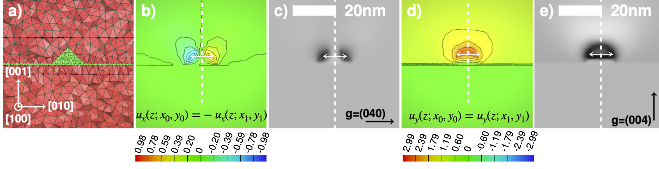

Fig. 2. Simulation of TEM images for pyramidal QD: a) QD geometry. b) and d) Different components of displacement field. c) and e) corresponding TEM images for strong beam conditions as indicated by the direction of the chosen vectors $\mathbf{g}$. Images from [3] used under CC-BY.

III. Symmetries in TEM images

The simulated TEM images in Fig. 2 c) and e) show a pixelwise symmetry, i.e. for two different pixels (x_0, y_0) and (x_1, y_1) we have the same intensities: $|\phi_{\mathbf{g}}(z_*; x_0, y_0)|^2 = |\phi_{\mathbf{g}}(z_*; x_1, y_1)|^2$. For Fig. 2 e) this in not surprising since for both pixels the profile of the corresponding vertical component of the displacement is the same, see Fig. 2 d). However, in Fig. 2 c) the profiles have opposite values, see Fig. 2 b). This observation raises the question whether this symmetry is a result of the specific strain profile or a general property of the imaging process. We approach this question by answering the following more general question: Which transformations $(A, F) \to (\tilde{A}, \tilde{F})$ give the same intensity?

By analysing the DHW equations mathematically we proved that in the two-beam approximation $\Lambda_2 = \{\mathbf{0}, \mathbf{g}'\}$ the following hold:

1) (Sign change) Under strong beam conditions, i.e. $s_{\mathbf{0}} = s_{\mathbf{g}'} = 0$, changing the sign of the strain $\big(F(z) \rightsquigarrow -F(z)\big)$ is a symmetry.
2) (Midplane reflection) Midplane reflection $\big(F(z) \rightsquigarrow F(z_* - z)\big)$ is a symmetry.
3) (Excitation error symmetry) Combination of the above, $\big(F(z) \rightsquigarrow -F(z_* - z)\big)$, is a symmetry, if in addition we change the sign of the excitation error $s_{\mathbf{g}'} \rightsquigarrow -s_{\mathbf{g}'}$.

These are properties of the imaging process and are independent of the shape of the strain profile. The sign change symmetry 1) directly explains the observation for Fig. 2 c). In Fig. 3 b) we see a series of TEM images of a spherical quantum dot, for different depths of the quantum dot and different excitation errors. The different symmetries observed here (colored boxes) can be explained by these three properties in combination with the shape of the strain profile. For example, from the excitation error symmetry 3) we can apply midplane reflection plus sign change of the strain, which for the odd strain profile in Fig. 3 c) corresponds to shifting the strain with respect to the center, and then change the sign of the excitation error. This explains the symmetric images in Fig. 3b) indicated by the green and red boxes.

For more examples we refer to [3], where the detailed proofs of these and additional symmetry properties, as well as an analysis in the case of absorption, can be found. A comprehensive mathematical analysis of the DHW equations can be found in [6]. The theory we developed allows us to distinguish between symmetries of the imaging process and symmetries of the strain field. This can be used to extract information for the inclusion, e.g. shape or size, as well as to imaging of dislocations, since the TEM images are sensitive to the strain field induced by the dislocation.

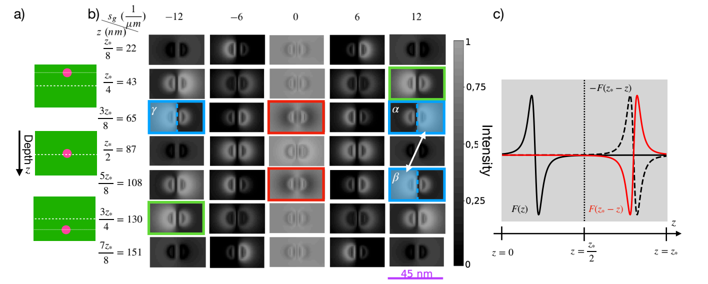

Fig. 3. Symmetries between images: a) Schematics of the position of the quantum dot b) Series of TEM images for a spherical quantum dot for varying positions and excitation errors: For $s_{\mathbf{g}} = 0$ the images are pixelwise symmetric with respect to the center (red boxes). For $s_{\mathbf{g}} \neq 0$ they are symmetric if in addition the sign of the excitation error is changed (green boxes). The images are mirrored to each other with respect to the center for the same excitation error (α and β blue boxes) or with respect to the sign of the excitation error for a fixed position (α and γ blue boxes). Adapted from [7] used under CC-BY. c) Plot of a shifted odd function $F(z)$ (black) and the midplane reflection of it (red) illustrating that shifting (black dotted) needs an additional sign change to correspond to midplane reflection. Adapted from [3] used under CC-BY.

Acknowledgment

The authors are grateful to Tore and Laura Niermann for the helpful discussions.

References

[1] A. Maltsi, T. Niermann, T. Streckenbach, K. Tabelow, and Th. Koprucki, “Numerical simulation of TEM images for In(Ga)As/GaAs quantum dots with various shapes,” Opt. Quant. Electron., vol. 52, 2020
[2] AP. Pogany, PS. Turner, “Reciprocity in electron diffraction and microscopy,” Acta Crystallogr. Sect. A 24, 103–109, 1968
[3] Th. Koprucki, A. Maltsi, and A. Mielke, “ Symmetries in transmission electron microscopy imaging of crystals with strain,” Proc. R. Soc. A., vol. 478, 2022
[4] M. D. Graef, “Introduction to conventional transmission electron microscopy,” Cambridge University Press, 2003
[5] Th. Koprucki, A. Maltsi, and A. Mielke, “On the Darwin-Howie-Whelan equations for the scattering of fast electrons described by the Schrödinger equation,” SIAM Journal on Applied Mathematics, vol. 81, 2021,
[6] A. Maltsi, “A mathematical study of the Darwin-Howie-Whelan equations for Transmission Electron Microscopy”, Doctoral Thesis, Humboldt-Universität zu Berlin, 2023
[7] L. Niermann, “Untersuchung und Anwendung der dynamischen Beugung an inhomogenen Verschiebungsfeldern in Elektronenstrahlrichtung in Halbleiterheterostrukturen,”, Doctoral Thesis, Technische Universität Berlin, 2021